Supplementary materials for:

Effect Analysis of the Digital Spectrometer FFT Algorithm on THz Atmospheric Limb Sounder (TALIS) System Sensitivity

Haowen Xu [1,2], Hao Lu [1], Zhenzhan Wang [1], Wenming He [1,2], Wenyu Wang [1]

[1] Key Laboratory of Microwave Remote Sensing, National Space Science Center, Chinese Academy of Sciences, Beijing 100190, China;

[2] University of Chinese Academy of Sciences, Beijing 100049, China

Content of this file

Figures S1 to S9

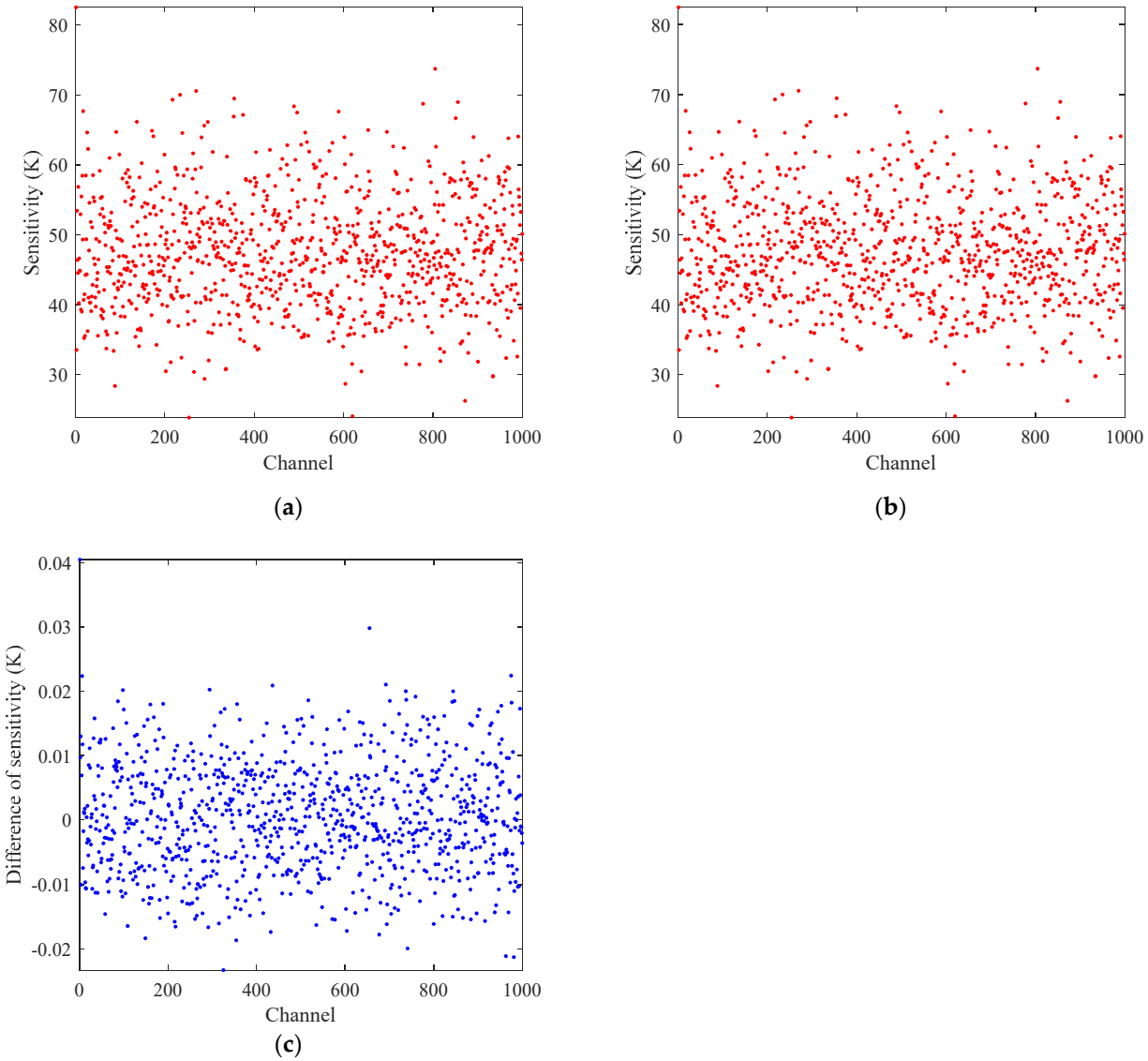

Figure S1. The sensitivity obtained by the S-FFT-C method and the S-FFT-R method after one of the simulations at the integration time of 0.5 ms: (**a**) S-FFT-C method; (**b**) S-FFT-R method; (**c**) difference of sensitivity between the two methods for each channel.

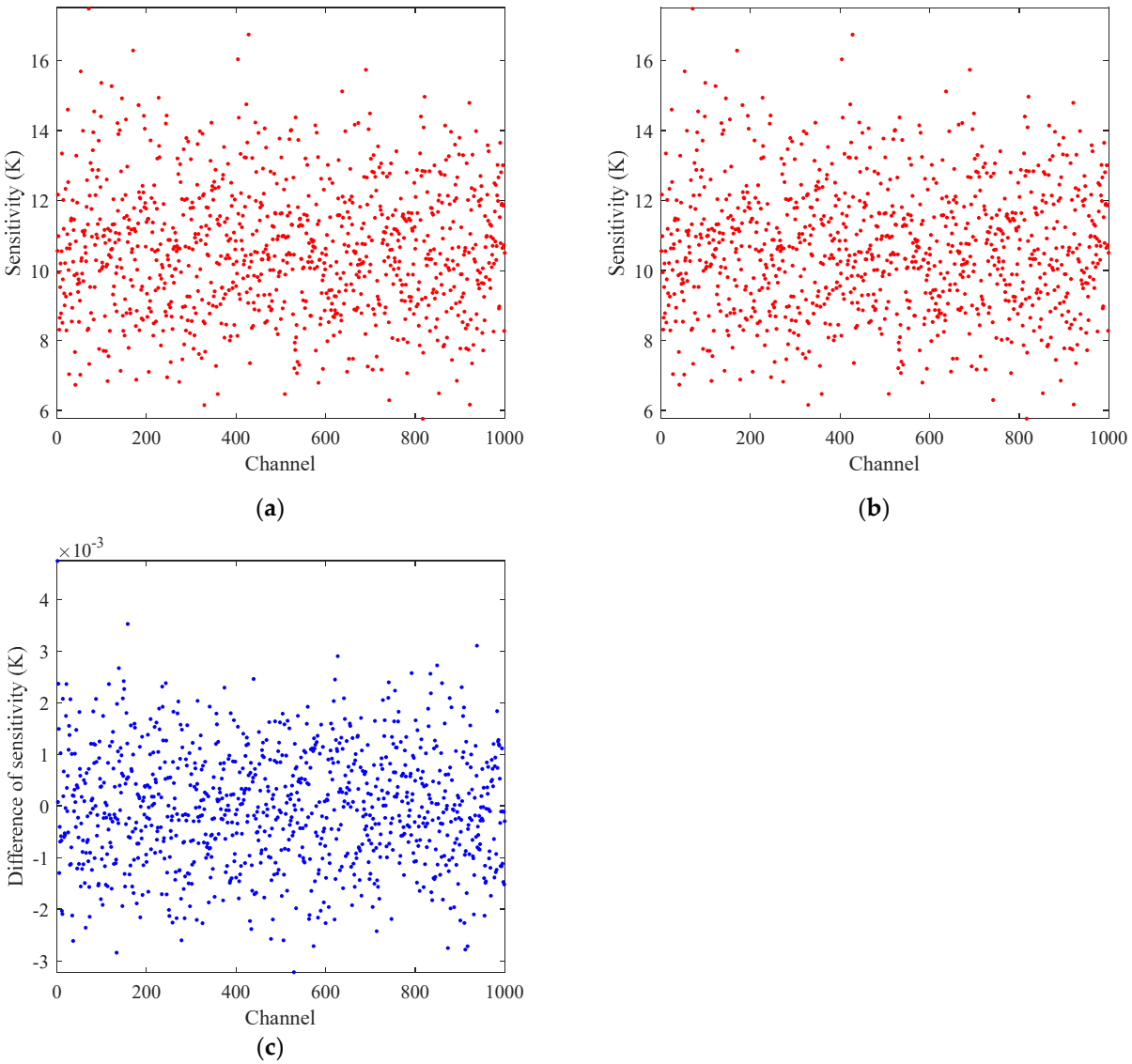

Figure S2. The sensitivity obtained by the S-FFT-C method and the S-FFT-R method after one of the simulations at the integration time of 10 ms: (**a**) S-FFT-C method; (**b**) S-FFT-R method; (**c**) difference of sensitivity between the two methods for each channel.

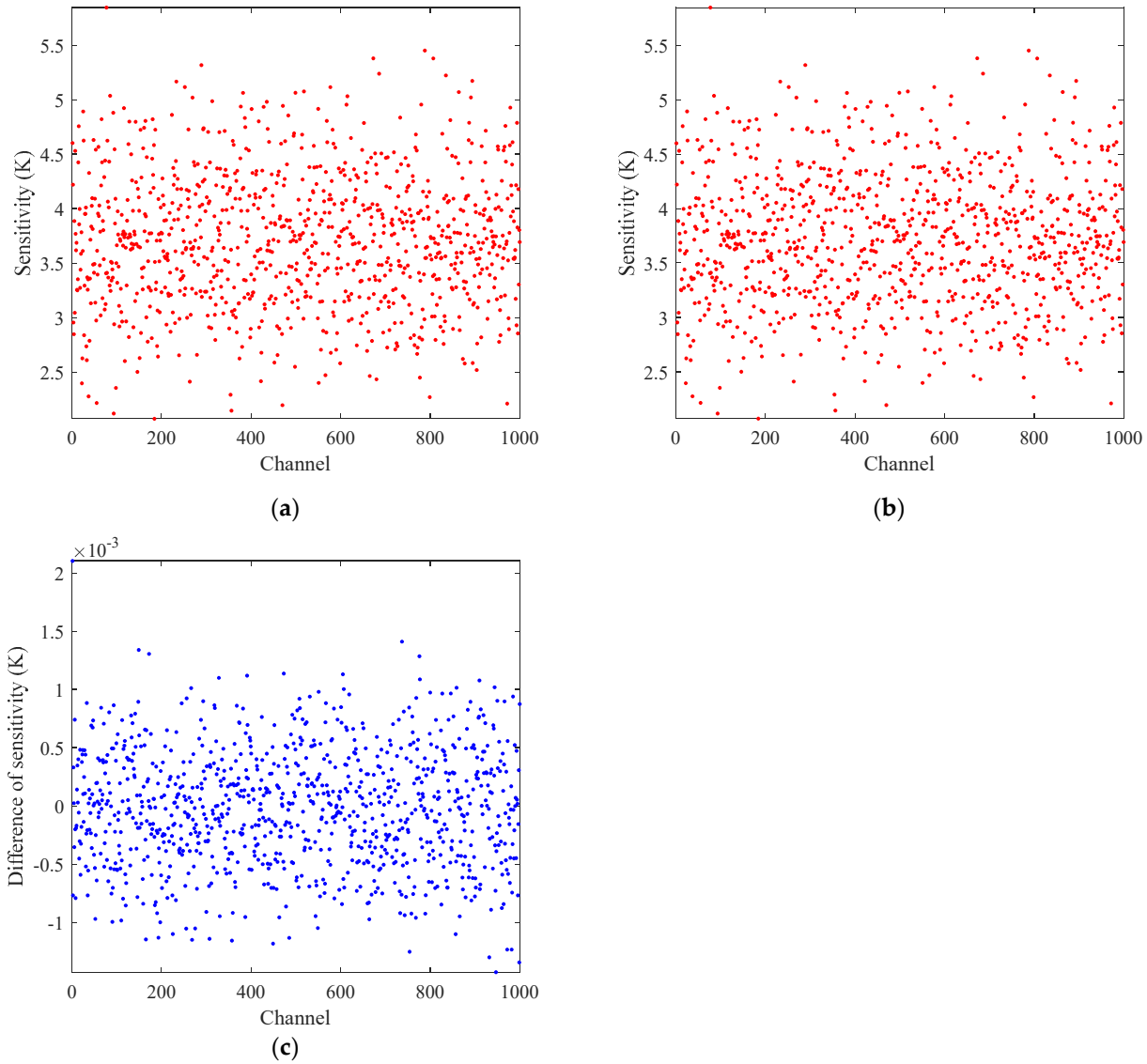

Figure S3. The sensitivity obtained by the S-FFT-C method and the S-FFT-R method after one of the simulations at the integration time of 80 ms: (**a**) S-FFT-C method; (**b**) S-FFT-R method; (**c**) difference of sensitivity between the two methods for each channel.

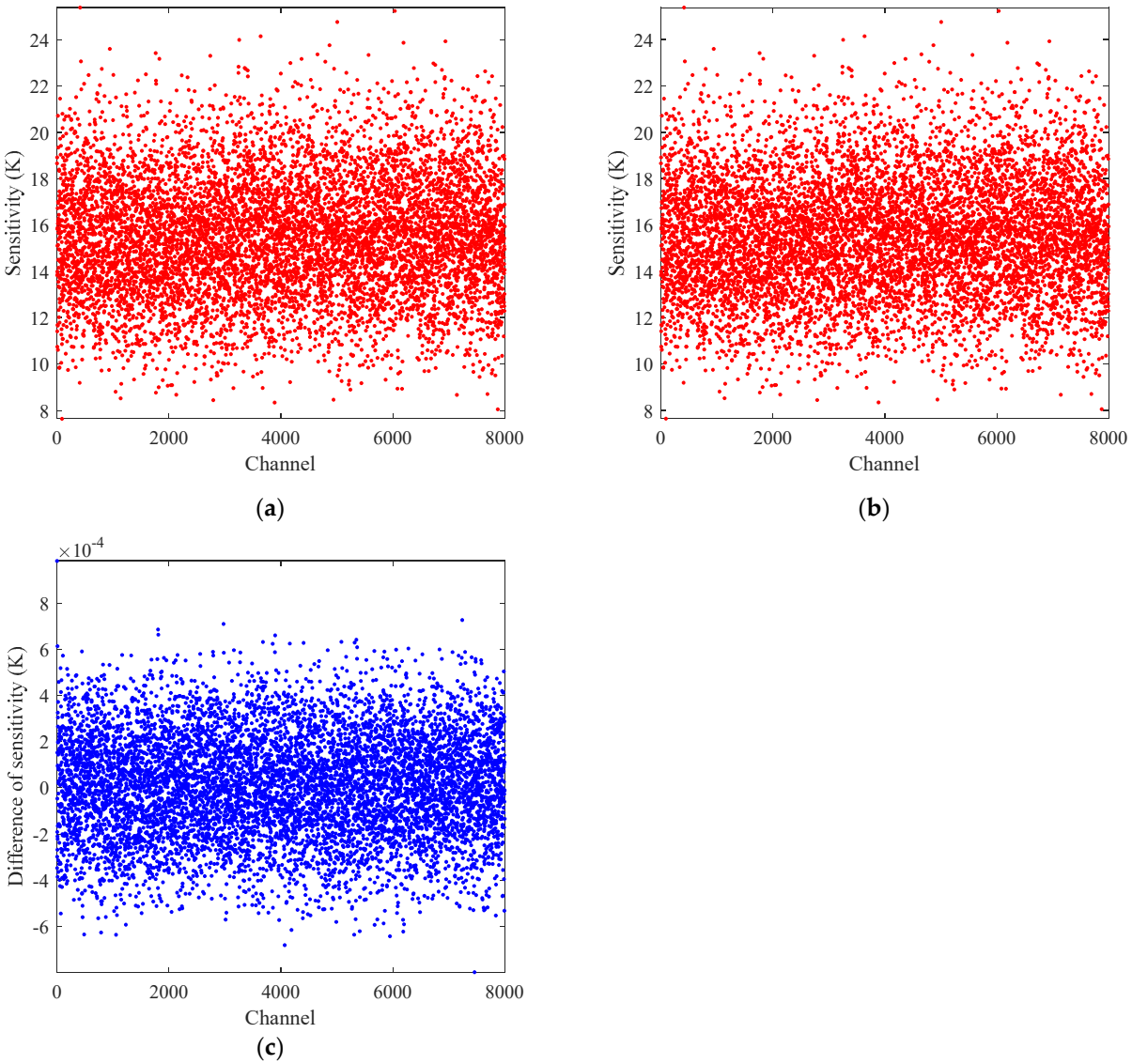

Figure S4. The sensitivity obtained by the S-FFT-C method and the S-FFT-R method after one of the simulations at the spectral resolution of 0.25 MHz: (a) S-FFT-C method; (**b**) S-FFT-R method; (**c**) difference of sensitivity between the two methods for each channel.

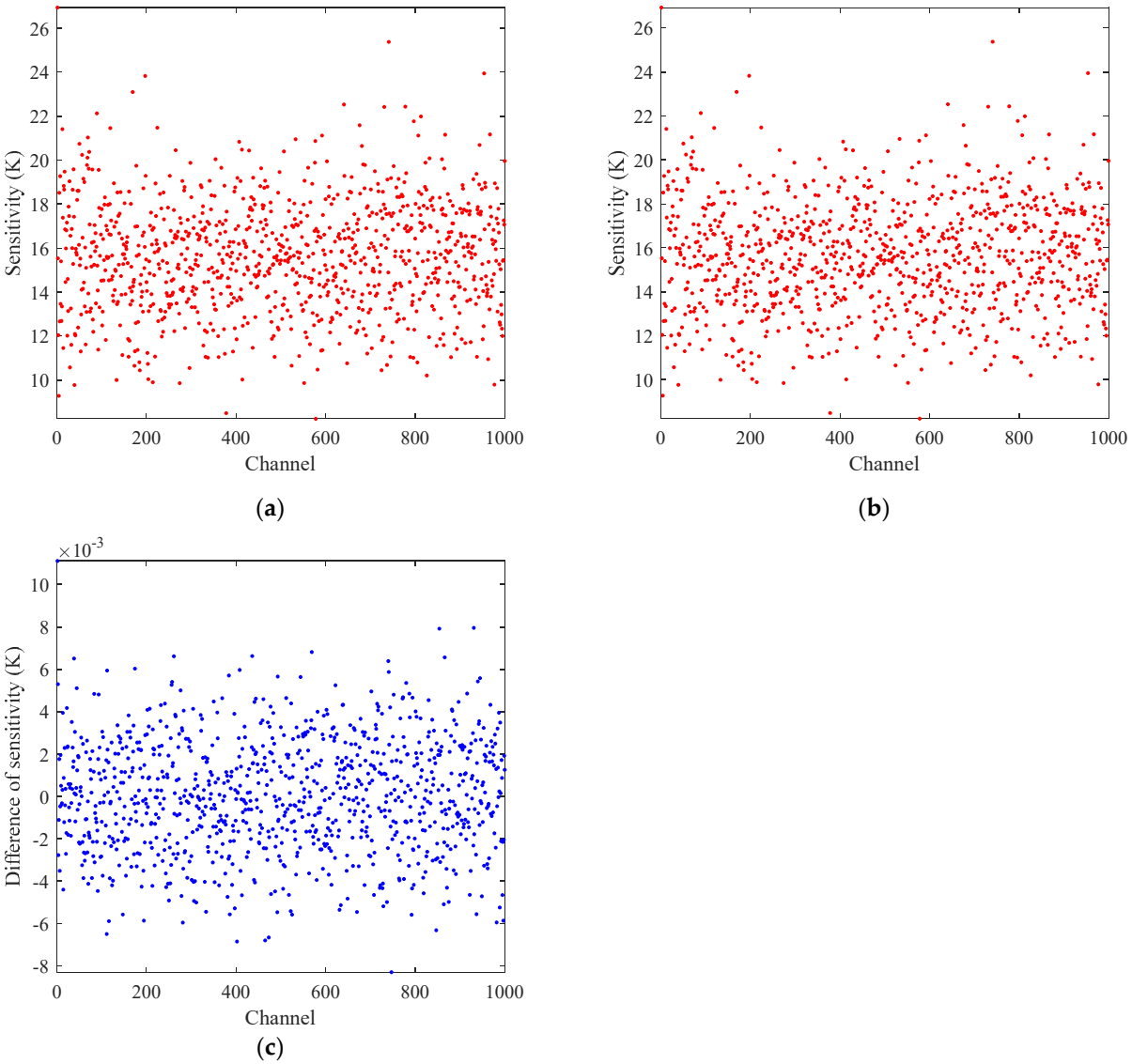

Figure S5. The sensitivity obtained by the S-FFT-C method and the S-FFT-R method after one of the simulations at the spectral resolution of 2 MHz: (a) S-FFT-C method; (**b**) S-FFT-R method; (**c**) difference of sensitivity between the two methods for each channel.

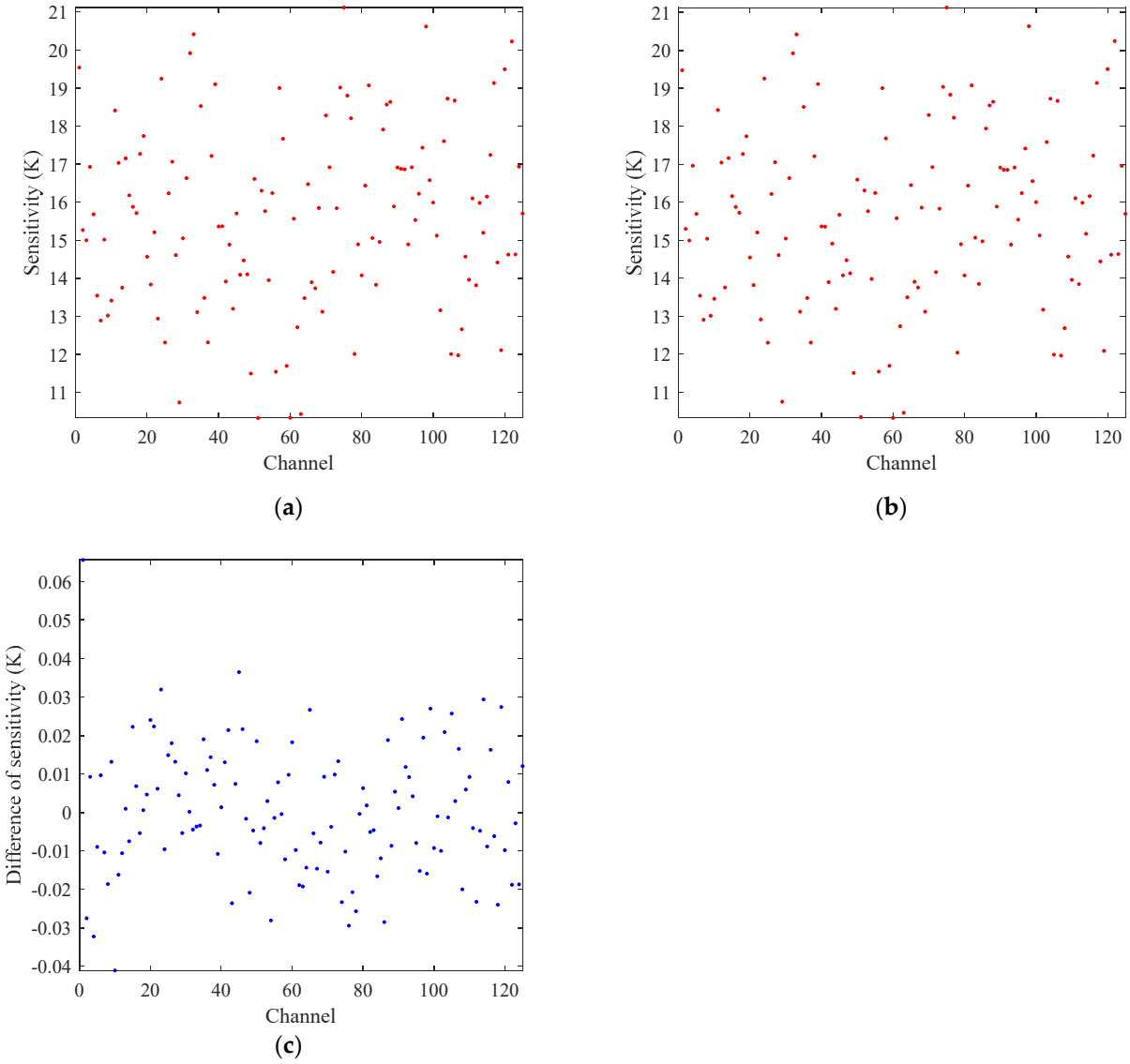

Figure S6. The sensitivity obtained by the S-FFT-C method and the S-FFT-R method after one of the simulations at the spectral resolution of 16 MHz: (a) S-FFT-C method; (**b**) S-FFT-R method; (**c**) difference of sensitivity between the two methods for each channel.

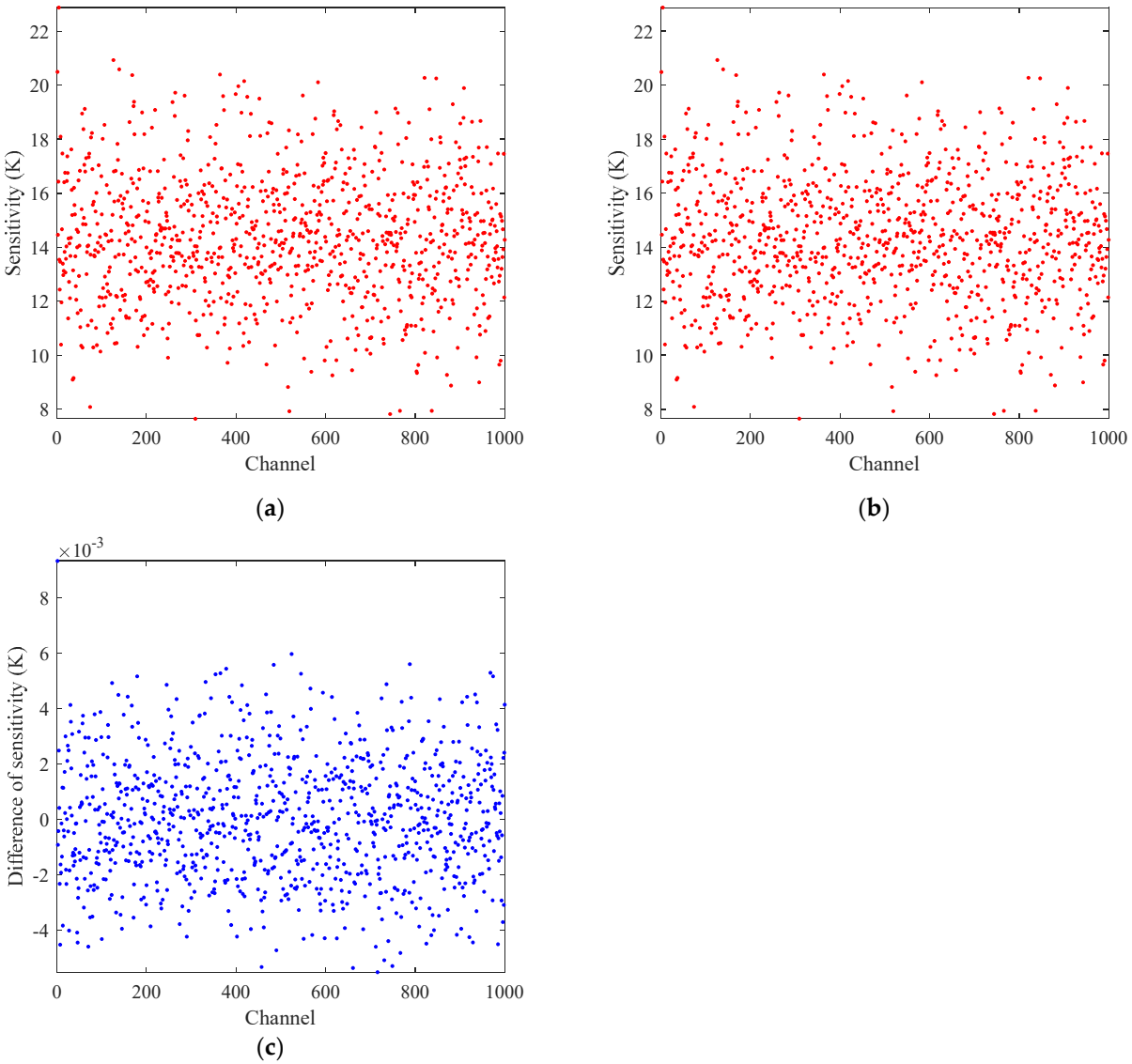

Figure S7. The sensitivity obtained by the S-FFT-C method and the S-FFT-R method after one of the simulations at the quantization bit of 3-bit: (a) S-FFT-C method; (b) S-FFT-R method; (c) difference of sensitivity between the two methods for each channel.

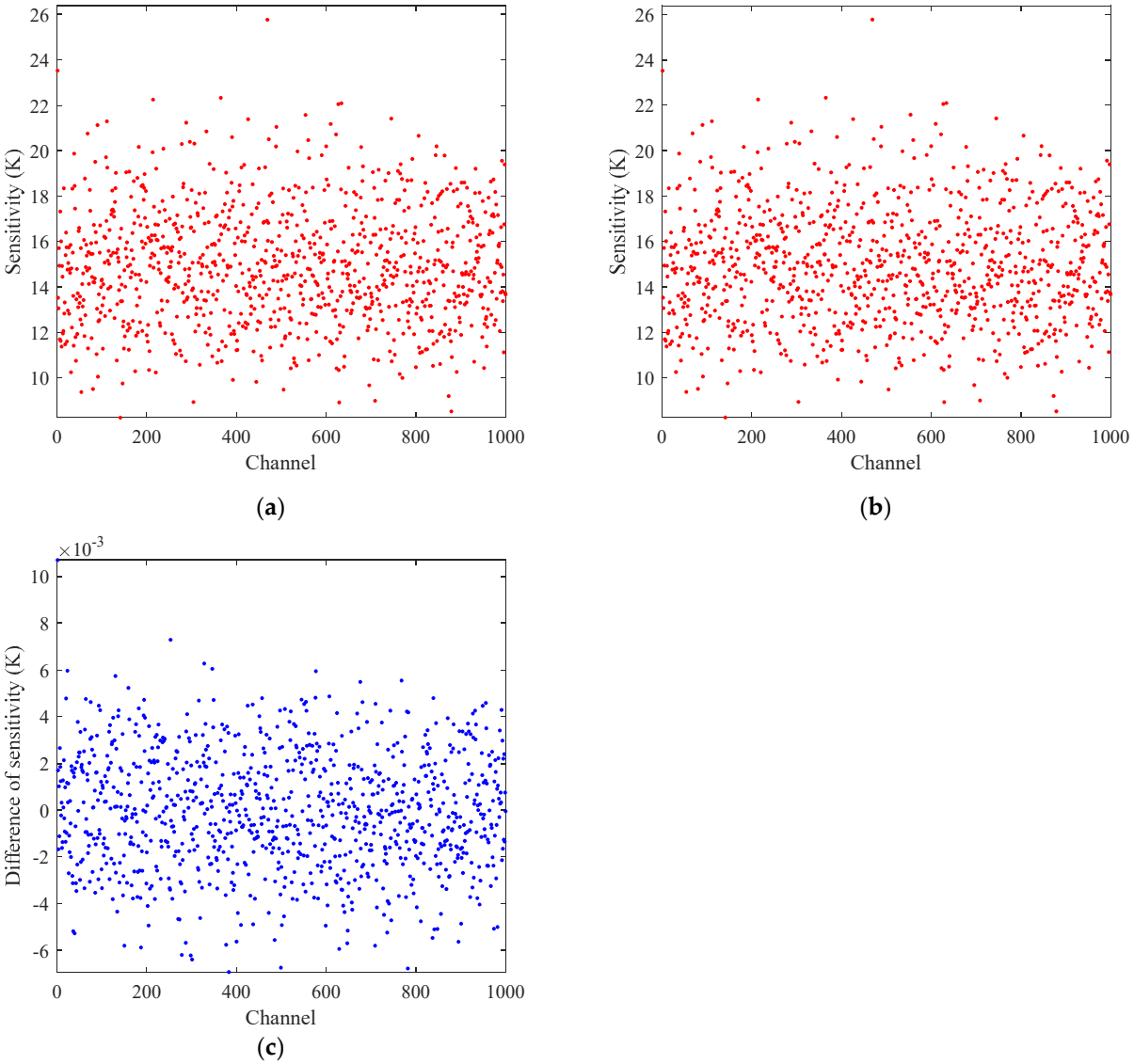

Figure S8. The sensitivity obtained by the S-FFT-C method and the S-FFT-R method after one of the simulations at the quantization bit of 6-bit: (a) S-FFT-C method; (b) S-FFT-R method; (c) difference of sensitivity between the two methods for each channel.

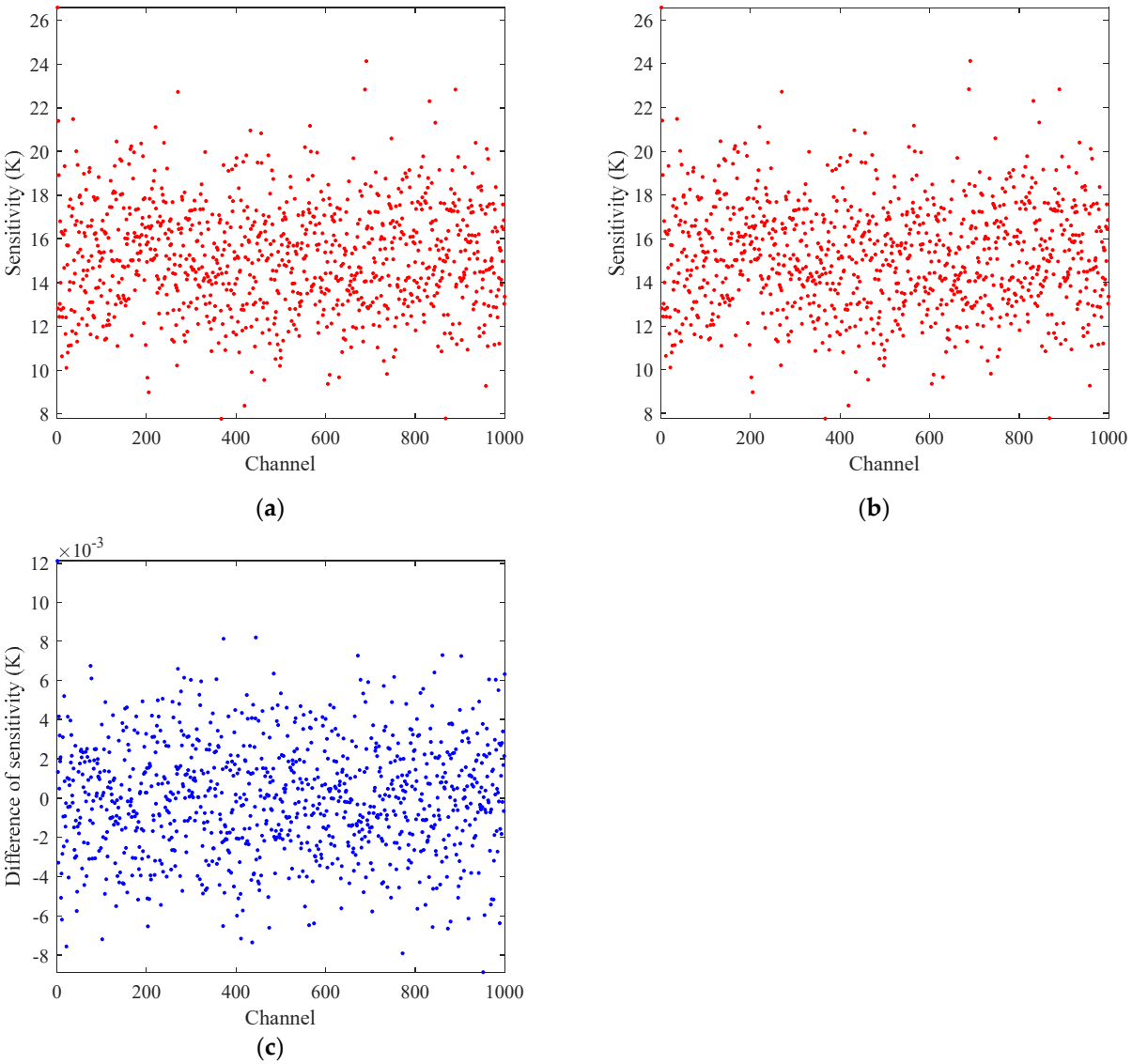

Figure S9. The sensitivity obtained by the S-FFT-C method and the S-FFT-R method after one of the simulations at the quantization bit of 12-bit: (a) S-FFT-C method; (b) S-FFT-R method; (c) difference of sensitivity between the two methods for each channel.